Modeling Li-ion Battery Capacity Depletion in a Particle Filtering Framework

Bhaskar Saha[1] and Kai Goebel[2]

[1]*Mission Critical Technologies, Inc. (NASA ARC), 2041 Rosecrans Avenue, Suite 220, El Segundo, CA 90245*
bhaskar.saha@nasa.gov

[2]*NASA Ames Research Center, Moffett Field, CA 95134, USA*
kai.goebel@nasa.gov

ABSTRACT

This paper presents an empirical model to describe battery behavior during individual discharge cycles as well as over its cycle life. The basis for the form of the model has been linked to the internal processes of the battery and validated using experimental data. Subsequently, the model has been used in a Particle Filtering framework to make predictions of remaining useful life for individual discharge cycles as well as for cycle life. The prediction performance was found to be satisfactory as measured by performance metrics customized for prognostics. The work presented here provides initial steps towards a comprehensive health management solution for energy storage devices.[*]

1 INTRODUCTION

Battery powered applications have permeated our lives today at every level, from tiny Bluetooth headsets to cameras, cell phones and laptops to hybrid and electric vehicles. Similarly, the consequences of the failure of a battery can have different levels of severity ranging from reduced performance to operational impairment and even to catastrophic failure. A good understanding of battery performance degradation can aid immensely in improving user satisfaction and overall reliability for such systems. The research presented in this paper addresses these issues by developing an empirical model for Li-ion battery capacity depletion and by using it in a Particle Filtering (PF) framework to predict the remaining useful life (RUL) of the battery for a given discharge cycle as well as for its cycle-life.

Particle Filters are a class of Sequential Monte Carlo methods that not only use the information available from system measurements but also incorporate any models available for system behavior. This technique also has the ability to tune non-stationary model parameters simultaneously with state estimation, which combined with the representation of state space as multiple weighted particles, makes it ideal for state tracking and prediction. In the PF approach, the system state is represented by a pdf approximated by a set of particles (points) representing sampled values from the unknown state space, and a set of associated weights denoting discrete probability masses. The particles are generated and recursively updated from a nonlinear process model (that describes the evolution in time of the system under analysis), a measurement model, a set of available measurements, and an *a priori* estimate of the state pdf.

2 MOTIVATION

Americans purchase nearly 3 billion batteries (dry-cells) every year. On average, each person in the US disposes of 8 batteries every year (PKIDs, 2009). A rechargeable battery can replace hundreds of single-use batteries over its life. Also, all batteries contain metals such as mercury, lead, cadmium, nickel and lithium, which may contaminate the environment if disposed of improperly, hence reducing consumption eases the strain on natural resources.

During Operation Iraqi Freedom, the Marines used 3,028 batteries per day, which was "half the requirement of the entire battlefield" (Fein, 2003). These were non-rechargeable cells that did not have a charge indicator. Navy Captain Clark Driscoll said he wasn't sure how much battery life was discarded inadvertently by changing batteries early. "[I'm] afraid to say that in the first several weeks we threw away a lot," he said. Lt. Cmdr. John LaTulip, of the U.S.

[*] This is an open-access article distributed under the terms of the Creative Commons Attribution 3.0 United States License, which permits unrestricted use, distribution, and reproduction in any medium, provided the original author and source are credited.

Central Command's maintenance branch, said, "If [soldiers] could get a device put on [the battery] that tells them what is left in the charge, then they could use those batteries to full capability. Right now we can't do that… [We are] looking at policy for using rechargeables and how do you program and plan for that."

Apart from the issue of increasing efficiency, and reducing cost and wastage, rechargeable batteries are a key enabling technology for solving energy problems of the future. One key feature of renewable energy sources like solar, wind, tidal, etc. is that they are not continually available. A report by the California ISO Board says, "Wind generation energy production is extremely variable, and in California, it often produces its highest energy output when the demand for power is at a low point" (CA ISO, 2008). An energy storage facility coupled with these power generation sources would make these solutions more economically viable. Such energy storages, comprising batteries, fuel cell or super-capacitors, would in turn need reliable health monitoring systems to ensure viable levels of system availability, reliability and sustainability and to protect the assets from degradation due to non-optimal usage. Finally, battery health management will also play a critical role in electric vehicles that will be dependant on an accurate gauge for remaining charge and for trade-offs in long-term durability and short-term usage needs.

3 BACKGROUND

The main purpose of modeling battery aging is to enable effective *battery health monitoring* (BHM) applications that ensure that the battery operation stays within design limits and to provide warning or mitigate damage when these limits are exceeded. Current BHM efforts come in many flavors, from the data-driven (Rufus *et al*., 2008) to the model-based (Plett, 2004) and even hybrid approaches (Goebel *et al*., 2008). Implementation complexity can range from intermittent manual measurements of voltage and electrolyte specific gravity to fully automated online supervision of various measured and estimated battery parameters using dynamic models. The sophistication of the models also varies from a collection of basis functions (Stamps *et al*., 2005) to detailed formulations derived from physical analysis of the cell (Hartley and Jannette, 2005).

Looking at the issue from the application perspective, researchers in the aerospace domain have examined the various failure modes of the battery subsystems. Different diagnostic methods have been evaluated, like discharge to a fixed cut-off voltage, open circuit voltage, voltage under load and electrochemical impedance spectrometry (EIS) (Vutetakis and Viswanathan, 1995). In the field of telecommunications, people have looked to combine conductance technology with other measured parameters like battery temperature/differential information and the amount of float charge (Cox and Perez-Kite, 2000).

Other works have concentrated more on the prognostic angle rather than the diagnostic one. Statistical parametric models have been built to predict time to failure (Jaworski, 1999). Electric and hybrid vehicles have been another fertile area for battery health monitoring (Meissner and Richter, 2003). Impedance spectroscopy has been used to build battery models for cranking capability prognosis (Blanke *et al*., 2005). State estimation techniques, like the Extended Kalman Filter (EKF), have been applied for real-time prediction of state-of-charge (SOC) and state-of-life (SOL) of automotive batteries (Bhangu *et al*., 2005; Plett, 2004). A decision-level fusion of data-driven algorithms, like Autoregressive Integrated Moving Average (ARIMA) and neural networks, has been investigated for both diagnostics and prognostics (Kozlowski, 2003). As the popular cell chemistries changed from lead acid to nickel metal hydride to lithium ion, cell characterization efforts have kept pace. Dynamic models for the lithium ion batteries that take into consideration nonlinear equilibrium potentials, rate and temperature dependencies, thermal effects and transient power response have been built (Gao *et al*., 2002; Hartmann II, 2008; Santhanagopalan *et al*., 2008).

However, there is still need for a flexible prognostics framework that combines the sensor data from battery monitors, the models developed, and the appropriate state estimation and prediction algorithms, in the form of an integrated BHM solution. The research described in this paper is an early step in this direction.

4 BATTERY CHARACTERISTICS

Batteries are essentially energy storage devices that facilitate the conversion, or *transduction*, of chemical energy into electrical energy, and vice versa (Huggins, 2008). They consist of a pair of *electrodes* (*anode* and *cathode*) immersed in an *electrolyte* and sometimes separated by a *separator*. The chemical driving force across the cell is due to the difference in the chemical potentials of its two electrodes, which is determined by the difference between the *standard Gibbs free energies* the products of the reaction and the reactants. The theoretical *open circuit voltage*, E^{o}, of a battery is measured when all reactants are at 25^{o}C and at 1M concentration or 1 atm pressure. However, this voltage is not available during use. This is due to the various passive components inside like the electrolyte, the

separator, terminal leads, etc. The voltage drop due to these factors can be mainly categorized as:

- *IR drop* – This drop in cell voltage is due to the current flowing across the internal resistance of the battery.
- *Activation polarization* – This term refers to the various retarding factors inherent to the kinetics of an electrochemical reaction, like the work function that ions must overcome at the junction between the electrodes and the electrolyte.
- *Concentration polarization* – This factor takes into account the resistance faced by the mass transfer (e.g. diffusion) process by which ions are transported across the electrolyte from one electrode to another.

Figure 1 depicts the typical polarization curve of a battery with the contributions of all three of the above factors shown as a function of the current drawn from the cell. Since, these factors are current-dependent, i.e. they come into play only when some current is drawn from the battery, the voltage drop caused by them usually increases with increasing output current.

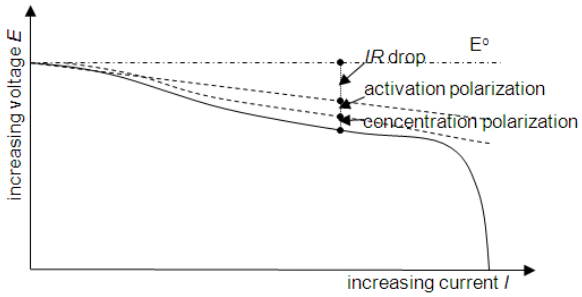

Figure 1: Typical polarization curve of a battery.

Since the output current plays such a big role in determining the losses inside a battery, it is an important parameter to consider when comparing battery performance. The term most often used to indicate the rate at which a battery is discharged is the *C-Rate* (Huggins, 2008). The discharge rate of a battery is expressed as *C*/*r*, where *r* is the number of hours required to completely discharge its nominal capacity. So, a 2 Ah battery discharging at a rate of *C*/10 or 0.2 A would last for 10 hours. The terminal voltage of a battery, as also the charge delivered, can vary appreciably with changes in the C-Rate. Furthermore, the amount of energy supplied, related to the area under the discharge curve, is also strongly C-Rate dependent. Figure 2 shows the typical discharge of a battery and its variation with C-Rate. Each curve corresponds to a different C-Rate or *C*/*r* value (the lower the *r* the higher the current) and assumes constant temperature conditions.

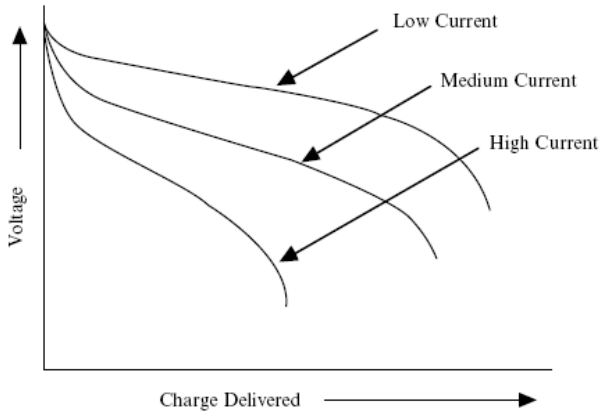

Figure 2: Schematic drawing showing the influence of the current density upon the discharge curve. (Reproduced from Figure 1.14 in (Huggins, 2008)).

Moving on from the theoretical aspects to the application point of view, the relevant physical properties of a battery may be different in different cases. Sometimes *specific energy* and *specific power* (energy and power available per unit weight) are important, as in vehicle propulsion applications. Other times the amount of energy stored per unit volume, called the *energy density*, can be more important for batteries that power portable electronic devices, like cell-phones, laptop computers, cameras, etc., while power per unit volume, known as *power density*, can be important for some uses like cordless power tools. However, in recent times when the use of rechargeable batteries is proliferating in consumer products, an important parameter to consider is *cycle life*, which is the number of times a battery can be recharged before its capacity has faded beyond acceptable limits (typically ~20-30%).

The degradation of battery capacity with aging, as encapsulated by the cycle life parameter, can be modeled by the concept of *Coulombic efficiency*, η_C, defined as the fraction of the prior charge capacity that is available during the following discharge cycle (Huggins, 2008). This depends upon a number of factors, especially current and depth of discharge in each cycle. The temperature at which batteries are stored and operated under also has a significant effect on the Coulombic efficiency. Figure 3 shows the degradation of battery capacity with cycling for different values of Coulombic efficiency. Notice how even a small inefficiency factor of 0.5% (Coulombic efficiency = 0.995) can reduce the capacity by about 60% within 100 cycles.

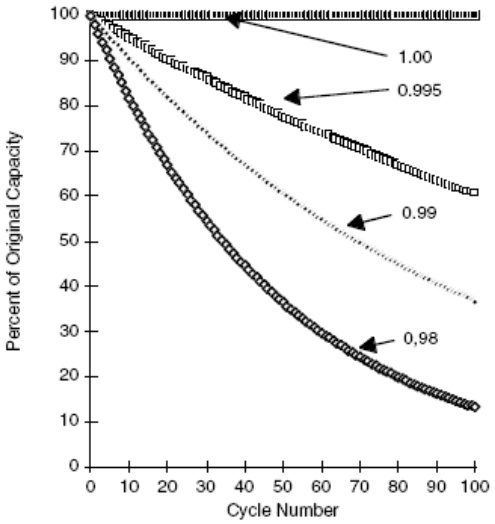

Figure 3: Influence of Coulombic efficiency upon available capacity during cycling. (Reproduced from Figure 1.8 in (Huggins, 2008)).

5 LI-ION PROPERTIES

There are several rechargeable battery technologies available on the market right now, each having distinct characteristics. However, Li-ion batteries are becoming increasingly popular for a variety of applications, from consumer electronics to power tools, to electric vehicles and even to space applications. Li-ion batteries have a number of important advantages over competing technologies (Huggins, 2008):

- Since the electrodes of a Li-ion battery are made of lightweight lithium and carbon, they are usually lighter than other types of rechargeable batteries of the same size. Lithium is also a highly reactive element; hence a lot of energy can be stored in its atomic bonds. This translates into a very high energy density for Li-ion batteries as compared to other chemistries like lead-acid or NiCd (nickel-cadmium) or NiMH (nickel-metal hydride).

- They have a low *self-discharge* rate, meaning that they hold their charge for longer periods of time. Self-discharge is caused by the residual ionic and electronic flow through a cell even when there is no external current being drawn.

- They have no *memory effect*, which means that Li-ion batteries do not have to be completely discharged before recharging in order to retain full charge capacity, as with some battery chemistries like NiCd.

- Li-ion batteries have a long cycle life. They can handle hundreds of charge and discharge cycles without significant degradation of their capacity.

However, they have a few disadvantages as well (Buchmann, 2001; Huggins, 2008):

- The service life or shelf life of a Li-ion battery decreases with aging even if it is not used unlike other chemistries. This means that from the time of manufacturing, regardless of the number of times it was cycled, the capacity of a Li-ion battery will decline gradually. This is due to an increase in internal resistance, which makes the problem more pronounced in high-current applications than low-current ones.

- They are more sensitive to high temperatures than most other chemistries. Hot storage and operating conditions causes Li-ion battery packs to degrade much faster than they normally would.

- Li-ion batteries can be severely damaged by *deep discharge*, i.e. by discharging them below the minimum voltage threshold recommended by the manufacturer (usually 2.7 V for a single cell). Consequently, Li-ion battery packs come with an on-board circuit to manage the battery. This makes them even more expensive than they already are.

- In general Li-ion chemistry is not as safe as NiCd or NiMH. This is because the anode produces heat during use, while the cathode produces oxygen (not for all Li-ion chemistries). Lithium being highly reactive can combine with this oxygen, leading to the possibility of the battery catching on fire.

Considering both the advantages and the drawbacks, Li-ion batteries seem one of the more important battery technology for the present and the future. It is for this reason that we chose them for our battery prognostics research.

6 MODELING APPROACH

Modeling a Li-ion battery from the first principles of the internal electrochemical reactions can be very tedious and computationally intractable. Hence, we take the approach of representing the various losses inside a battery, like the IR drop, activation polarization and concentration polarization, as impedances in a lumped parameter model (Figure 4). The IR drop due to the *electrolyte resistance* is denoted as R_E. The

activation polarization is modeled as a *charge transfer resistance* R_{CT} and a *dual layer capacitance* C_{DL} in parallel, while the concentration polarization effect is encapsulated as the *Warburg impedance* R_W.

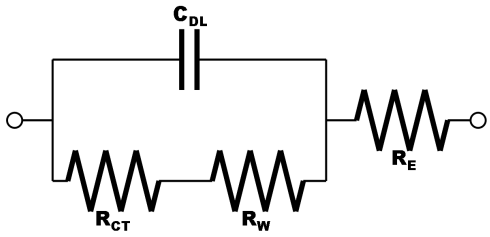

Figure 4: Lumped parameter model for a Li-ion battery (reproduced from Figure3 in (Goebel *et al*., 2008)).

This lumped parameter model may be analyzed in the time domain to derive the *discharge curves* of the battery or in the frequency domain to derive the *Nyquist plots*. The latter can be achieved by EIS measurements, and the plots can subsequently be used to reason about the internal degradation processes. However, EIS measurements require specialized equipment and measurement conditions that prevent them from being widely used in everyday applications. For the purposes of this paper we will disregard the frequency domain analysis and concentrate on the time domain aging characteristics of the battery.

6.1 End-of-discharge

As mentioned earlier, the goal of this research is to predict the RUL for any given discharge cycle of the battery as well as the cycle life. This is a two-part problem with different physical processes affecting the RUL prediction for the end-of-discharge (EOD) and end-of-life (EOL). To tackle the EOD problem, we need to predict the way the impedance parameters change with charge depletion during the discharge cycle. Since the impedance parameters are essentially representations of electrochemical reactions and transport processes inside the battery, they are strongly affected by the internal temperature of the battery, the current load and the ionic concentrations of the reactants. We postulate that as discharge progresses the heat generated by the reactions and the current flow causes the internal temperature to go up, effectively increasing the mobility of the ions in the electrolyte, thus decreasing R_W. Decreasing R_W, however, increases the self-discharge rate, effectively increasing the electrolyte resistance R_E of the battery. Also, the increase in temperature results in faster consumption of the cell reactants causing them to be used up rapidly near the end of the discharge resulting in an increase in R_{CT} and a sharp drop in the cell voltage. EOD is reached when the output voltage hits the minimum safe voltage threshold, E_{EOD}, of the cell. For a cell current of I, the output voltage E is given by:

$$E = E^o - I(R_E + R_{CT} + R_W). \quad (1)$$

The variations in E^o with internal temperature (Hartmann II, 2008) are not explicitly modeled, but accounted for by the adaptive powers of the PF framework described later. For the empirical charge depletion model considered here, we express the output voltage in terms of the effects of the changes in the internal parameters:

$$E(t) = E^o - \Delta E_{sd}(t) - \Delta E_{rd}(t) - \Delta E_{mt}(t), \quad (2)$$

where, t is the time variable during a discharge cycle, ΔE_{sd} is the drop due to self-discharge, ΔE_{rd} is the drop due to cell reactant depletion and ΔE_{mt} denotes the voltage drop due to internal resistance to mass transfer (diffusion of ions). These individual effects are modeled as:

$$\Delta E_{sd}(t) = \alpha_1 \exp(-\alpha_2/t), \quad (3)$$

$$\Delta E_{rd}(t) = \alpha_3 \exp(\alpha_4 t), \quad (4)$$

$$\Delta E_{mt}(t) = \Delta E_{init} - \alpha_5 t, \quad (5)$$

where, ΔE_{init} is the initial voltage drop when current I flows through the initial value of the internal resistance R_E at the start of the discharge cycle, and $\boldsymbol{\alpha} = \{\alpha_1,\alpha_2,\alpha_3,\alpha_4,\alpha_5\}$ represents the set of model parameters to be estimated from the data. Figure 5 shows how the different voltage drop components defined in eqns. (3)-(5) combine to give the Li-ion discharge profile.

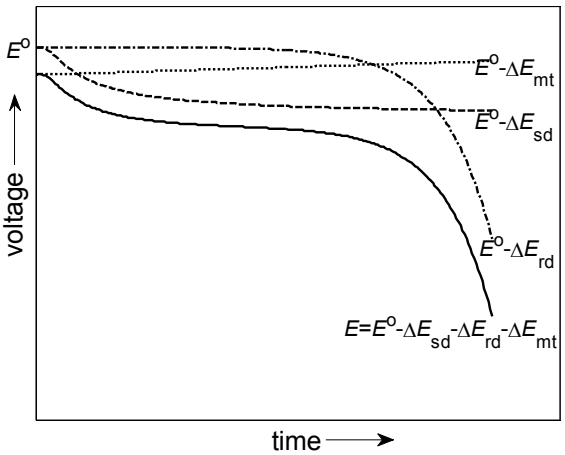

Figure 5: Decomposition of the Li-ion discharge profile in to different components.

6.2 End-of-life

In order to effectively determine the EOL of a Li-ion battery, we need to understand how the different operational modes, namely charge, discharge and rest, influence the charge capacity, C. The aging model presented in (Hartmann II, 2008) considers only the reduction in capacity with usage while neglecting the effects of rest periods. The use of a smoothing filter on the capacity measurements also reduces the fidelity of the prediction scheme.

In the work presented here, the combined effect of charge and discharge cycles is captured by the Coulombic efficiency factor η_C, as described in Section 4. The remaining factor that needs to be accounted for is the *self-recharge* during rest. In any battery, reaction products build up around the electrodes and slow down the reaction (HowStuffWorks, 2000). By letting the battery rest, the reaction products have a chance to dissipate, thus increasing the available capacity for the next cycle. For our empirical model, we represent this self-recharge as an exponential process, as suggested by data. The equation for battery aging can then be written as:

$$C_{k+1} = \eta_C\, C_k + \beta_1 \exp(-\beta_2/\Delta t_k), \qquad (6)$$

where, C_k denotes the charge capacity of the kth cycle, Δt_k is the rest period between cycles k and k+1, and β_1 and β_1 are the model parameters to be determined. Figure 6 shows the validity of equations (2)-(6) in modeling the discharge and self-recharge processes for an actual Li-ion battery cycle. Although the model is used to estimate the cell voltage during the self-recharge process in Figure 6, we assume the SOC of the battery to be correlated enough to the voltage during rest or *relaxation* periods (Huggins, 2008), when no external current is being drawn, so as to maintain the exponential functional form.

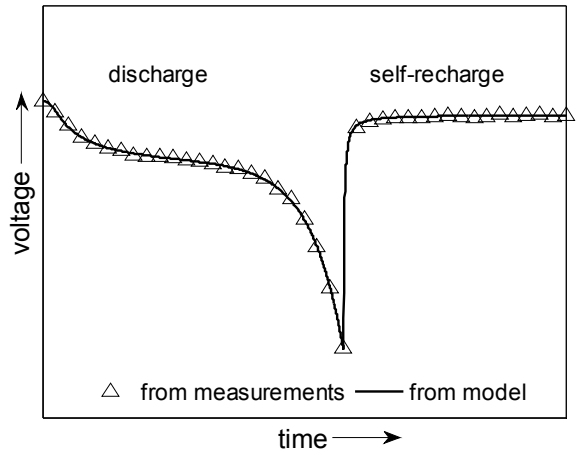

Figure 6: Model fit for Li-ion discharge and self-recharge processes.

7 PARTICLE FILTERING FRAMEWORK

The formulation of a model, though, is just a part of the solution. As mentioned above there are a number of unknown parameters that need to be identified. Even after identification, they may not be directly applicable to the test set since the values may differ from one battery to another, or for the same battery from one cycle to the next. Furthermore, for any given cycle the parameter values may be non-stationary. In general, given a model, the task of tracking a state variable and predicting future values is usually cast as a *filtering* problem. The variety of filtering techniques published in literature is enormous with each having performance advantages over others depending upon the application. For our task of battery prognostics, comprising the prediction of EOD and EOL, we need to reconcile our method with non-exact non-linear non-stationary models with non-Gaussian noise. Particle Filtering provides us a viable framework that allows us to explicitly represent and manage the uncertainties inherent to our problem.

Particle Filters (Gordon *et al*., 1993) are a novel class of non-linear filters that combine Bayesian learning techniques with importance sampling to provide good state tracking performance while keeping the computational load tractable. The idea is to represent the system state (in this case the battery SOC or voltage or capacity) as a probability density function (pdf) that is approximated by a set of particles (points) representing sampled values from the unknown state space, and a set of associated weights denoting discrete probability masses. The particles are generated from an *a priori* estimate of the state pdf, propagated through time using a nonlinear process model, and recursively updated from measurements through a measurement model. The main advantage of PFs here is that model parameters can be included as a part of the state vector to be tracked, thus performing model identification in conjunction with state estimation (Saha *et al*., 2009). After the model has been tuned to reflect the dynamics of the specific system being tracked, it can then be used to propagate the particles till the failure (e.g. EOD or EOL) threshold to give the RUL pdf (Saha *et al*., 2009).

In the case of our application, the EOD estimation problem is cast in the PF framework as follows:

$$\textbf{\textit{State transition model}} \equiv$$
$$\alpha_{j,i+1} = \alpha_{j,i} + \omega_{j,i}\,, \forall j = 1,\ldots,5,$$
$$E_{i+1} = E_i - \{\alpha_{1,i}\,\alpha_{2,i} \exp(-\alpha_{2,i}/t_i)/t_i^2 - \alpha_{3,i}\,\alpha_{4,i} \exp(\alpha_{4,i}\,t_i) - \alpha_{5,i}\}/f_s + \omega_i\,, \qquad (7)$$

$$\textbf{\textit{Measurement model}} \equiv \tilde{E}_i = E_i + v_i, \qquad (8)$$

where, i is the time index, f_s is the sampling frequency, $\tilde{E}_i$ denotes the measured cell voltage at time

index i, and $\omega_{j,i}$ ($\forall j$ = 1,…,5,), ω_i and v_i are independent zero-mean Gaussian noise terms.

The EOL estimation problem is similarly cast as:

$$\textbf{\textit{State transition model}} \equiv \begin{aligned} &\beta_{j,k+1} = \beta_{j,k} + \varphi_{j,k}\,,\ j = 1,2, \\ &C_{k+1} = \eta_C\, C_k + \beta_{1,k} \exp(-\beta_{2,k}/\Delta t_k) + \varphi_k\,, \end{aligned} \quad (9)$$

$$\textbf{\textit{Measurement model}} \equiv \tilde{C}_k = C_k + \psi_k\,, \quad (10)$$

where, k is the cycle index, $\tilde{C}_k$ denotes the charge capacity measured (as the integral of current over discharge time until cell voltage reaches E_{EOD}) at cycle index k, and $\varphi_{1,k}$, $\varphi_{2,k}$, φ_k and ψ_k are independent zero-mean Gaussian noise terms. The first term on the right hand side in the second line of equation (9) takes care of the Coulombic efficiency factor while the second term models the capacity gain due to rest.

Note that in both state equations (7) and (9) we have included the model parameter as part of the state vector, so that the PF can perform model identification in conjunction with state tracking.

8 RESULTS

The data used to validate the above approach have been collected from a custom built battery prognostics testbed (shown in Figure 7) at the NASA Ames Prognostics Center of Excellence (PCoE). This testbed comprises:

- Commercially available Li-ion 18650 sized rechargeable batteries,
- Programmable 4-channel DC electronic load,
- Programmable 4-channel DC power supply,
- Voltmeter, ammeter and thermocouple sensor suite,
- Custom EIS equipment,
- Environmental chamber to impose various operational conditions,
- PXI chassis based DAQ and experiment control, and
- MATLAB based experiment control, data acquisition and prognostics algorithm evaluation setup.

Figure 7: Battery prognostics testbed at NASA Ames PCoE.

In this testbed Li-ion batteries were run through 3 different operational profiles (charge, discharge and EIS) at room temperature, 23 °C. Charging was carried out in a constant current (CC) mode at 1.5 A until the battery voltage reached 4.2 V and then continued in a constant voltage (CV) mode until the charge current dropped to 20 mA. Discharge was carried out at a constant current (CC) level of 2 A until the battery voltage fell to 2.7 V. Experiments with more realistic variable load currents are planned for later. As mentioned before the EIS measurements are not used for the purposes of the research presented here. Repeated charge and discharge cycles result in accelerated aging of the batteries. The experiments were stopped when the batteries reached the EOL criteria of 30% fade in rated capacity (from 2 Ah to 1.4 Ah). Due to the differences in *depth-of-discharge* (DOD), the duration of rest periods and intrinsic variability, no two cells have the same SOL at the same cycle index. The aim is to be able to manage this uncertainty, which is representative of actual usage, and make reliable predictions of RUL in both the EOD and EOL contexts. Although several (> 16) batteries were aged in this setup, we present the results from a single battery. The accuracy and precision of the predictions shown below is representative of the performance on the other batteries as well.

Figure 8 shows the EOD predictions generated by the PF algorithm for an arbitrarily selected discharge cycle of a Li-ion battery under test. The red solid line shows the measured cell voltage, while the green patch represents the envelope of the PF tracking performance. The battery model is tuned continuously until we reach one of the predetermined prediction points (denoted by blue asterisks), at which time we freeze the model and use it to extrapolate the particle distribution till the E_{EOD} threshold.

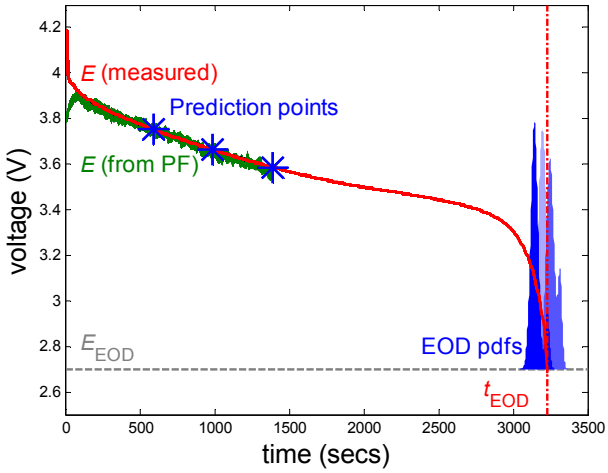

Figure 8: EOD prediction.

It is to be noted that we do not generate a single-valued prediction or a mean value with confidence bounds, but a full EOD pdf. Predictions are made at multiple points to test the robustness of the algorithm to model parameter drift. The pdfs generated have high accuracy and precision as can be seen from the overlap of the blue shaded areas to the right of Figure 8 and t_{EOD} marked by the vertical red broken line. Since the pdfs overlap each other, they are differentiated by varying shades of blue with the earliest one being the lightest and the later ones being progressively darker. Also, to improve visibility, the pdfs have been scaled by a factor of 50 and shifted to the E_{EOD} threshold.

In order to better quantify the prognostic performance, we calculate the α-λ performance metric, as defined in (Saxena *et al.*, 2008), for the prediction means computed as the weighted sum of the particle populations. We include several more prediction points in order to compute this metric, as shown by the blue asterisks in Figure 9. It can be seen that we achieve 90% accuracy (α = 0.1) right from the first prediction point onwards (λ = 0). This means that 500 seconds into the discharge, which is about 55 minutes long, we can predict the EOD point to within ±4 minute confidence limits. Halfway into the discharge we can predict to within ±2 minutes 45 seconds, and so on.

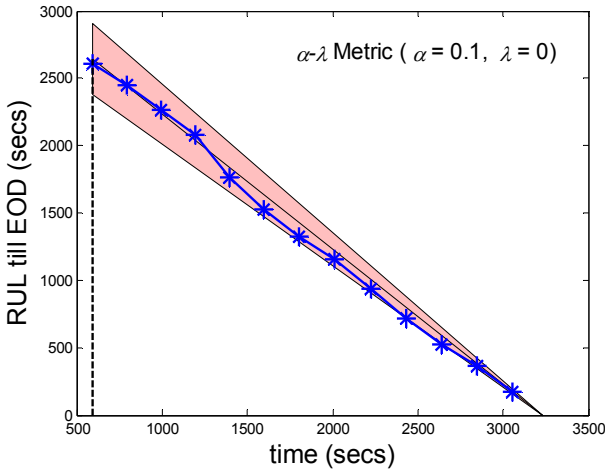

Figure 9: α-λ performance for EOD prediction.

The performance of the PF algorithm for EOL prediction problem is shown in Figure 10. The measured capacity values are shown by the red solid line, the PF tracking by the green patch and the prediction points by the blue asterisks. The EOL pdfs are denoted by the blue patches, lighter shades indicating earlier predictions. Note that modeling the capacity gain due to rest, as shown in equation (9), allows the PF to maintain track of the capacity during rests and make predictions accordingly. When predicting, the planned future usage and rest conditions are made available to the PF framework.

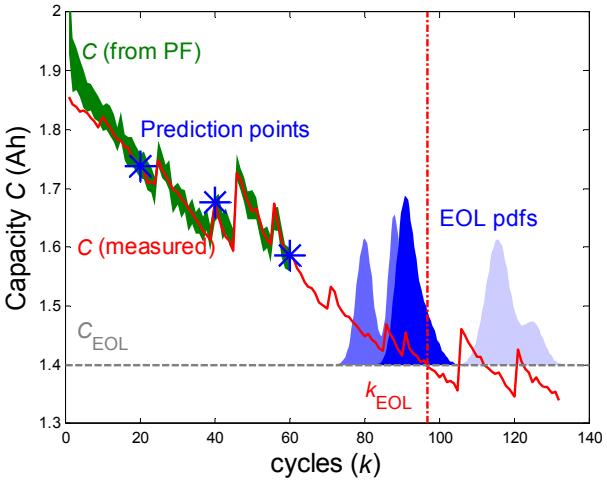

Figure 10: EOL prediction.

As can be seen, the EOL pdfs do overlap the cycles where the measured capacity crosses the EOL threshold of 1.4 Ah, however, due to the multiple crossings caused by the capacity gain during relaxation periods, the predictions keep shifting over them. Consequently, it is also difficult to compute convergence metrics like α-λ performance since it is difficult to define the true EOL. These issues are beyond the scope of this paper and will be tackled in future research. Figure 10, though, does demonstrate the viability of our PF based approach.

9 CONCLUSION

In summary, this paper lays out an empirical model to describe battery behavior during individual discharge cycles as well as over its cycle life. The basis for the form of the model has been linked to the internal processes of the battery and validated using experimental data. Subsequently, the model has been used in a PF framework to make predictions of EOD and EOL effectively. Although the model has been developed with Li-ion battery chemistries in mind, it can be applied to other batteries as long as effects specific to those chemistries are modeled as well (e.g. the memory effect in Ni-Cd rechargeable batteries).

The prediction results have been satisfactory so far, however, there remains considerable room for improvement. The model fidelity will improve when the influence of factors like temperature, discharge C-rate, DOD, SOC after charging, etc., are explicitly incorporated. This requires further intensive theoretical as well as experimental investigation of battery behavior. As the understanding of these factors improves, we will be able to better take advantage of advanced filtering techniques like unscented PF, Rao-Blackwellized PF (Saha *et al.*, 2009), and others, to further refine prognostic performance.

ACKNOWLEDGEMENT

The funding for this work was provided by the NASA Integrated Vehicle Health Management (IVHM) project under the Aviation Safety Program of the Aeronautics Research Mission Directorate (ARMD).

NOMENCLATURE

DOD	depth-of-discharge
EOD	end-of-discharge
EOL	end-of-life
RUL	remaining useful life
SOC	state-of-charge
SOL	state-of-life
C	charge capacity
I	load current
r	hours required to drain nominal capacity
η_C	Coulombic efficiency
R_E	electrolyte resistance
R_{CT}	charge transfer resistance
C_{DL}	dual-layer capacitance
R_W	Warburg resistance
t	time
i	time index
k	cycle index
E	cell voltage
E^o	theoretical open circuit voltage
ΔE_{sd}	voltage drop due to self-discharge
ΔE_{rd}	voltage drop due to reactant depletion
ΔE_{mt}	voltage drop due to mass transfer resistance
ΔE_{init}	initial voltage drop during discharge
$\alpha_{j=1,\ldots,5}$	EOD model parameters
$\beta_{j=1,2}$	EOL model parameters
Δt_k	rest period between cycles k and k+1
ω,ν,φ,ψ	zero-mean Gaussian noise terms
E_{EOD}	EOD voltage threshold (2.7 V)
t_{EOD}	time when E reaches E_{EOD}
C_{EOL}	EOL capacity threshold (1.4 Ah)
k_{EOL}	cycle when C reaches C_{EOL}

REFERENCES

(Bhangu *et al*., 2005) B. S. Bhangu, P. Bentley, D. A. Stone, and C. M. Bingham. Nonlinear Observers for Predicting State-of-Charge and State-of-Health of Lead-Acid Batteries for Hybrid-Electric Vehicles, *IEEE Transactions on Vehicular Technology*, vol. 54, no. 3, pp. 783-794, 2005.

(Blanke *et al*., 2005) H. Blanke, O. Bohlen, S. Buller, R. W. De Doncker, B. Fricke, A. Hammouche, D. Linzen, M. Thele, and D. U. Sauer. Impedance Measurements on Lead-acid Batteries for State-of-Charge, State-of-Health and Cranking Capability Prognosis in Electric and Hybrid Electric Vehicles, *Journal of Power Sources*, vol. 144, no. 2, pp. 418-425, 2005.

(Buchmann, 2001) I. Buchmann. *Will Lithium-Ion batteries power the new millennium?*, http://www.buchmann.ca/ Article5-Page1.asp.

(CA ISO, 2008) California ISO. 2008 Summer Loads and Resources Operations Preparedness Assessment, http://www.caiso.com/1fb7/1fb7855eed50.pdf.

(Cox and Perez-Kite, 2000) D. C. Cox and R. Perez-Kite. Battery State of Health Monitoring, Combining Conductance Technology with other Measurement Parameters for Real-time Battery Performance Analysis, *in Proceedings of 22nd International Telecommunications Energy Conference, INTELEC*, pp. 342-347, 2000.

(Fein, 2003) G. S. Fein. Battery Supplies Ran Dangerously Low in Iraq, *National Defense Magazine*, Sep 2003.

(Gao *et al*., 2002) L. Gao, S. Liu, and R. A. Dougal. Dynamic Lithium-Ion Battery Model for System Simulation, *IEEE Transactions on Components and Packaging Technologies*, vol. 25, no. 3, pp. 495-505, 2002.

(Goebel *et al*., 2008) K. Goebel, B. Saha, A. Saxena, J. R. Celaya, and J. Christophersen. Prognostics in Battery Health Management, *IEEE Instrumentation and Measurements Magazine*, vol. 11, no. 4, pp. 33–40, 2008.

(Gordon *et al*., 1993) N. J. Gordon, D. J. Salmond, and A. F. M. Smith (1993, April). Novel Approach to Nonlinear/Non-Gaussian Bayesian State Estimation, *Radar and Signal Processing*, *IEE Proceedings F*, vol. 140, no. 2, pp. 107-113, 1993.

(Hartley and Jannette, 2005) T. Hartley and A. G. Jannette. A First Principles Model for Nickel-Hydrogen Batteries, *in Proceedings of American Institute of Aeronautics and Astronautics' 3rd International Energy Conversion Engineering Conference*, San Francisco, CA, Aug 2005.

(Hartmann II, 2008) R. L. Hartmann II. *An Aging Model for Lithium-Ion Cells*, PhD dissertation, University of Akron, 2008.

(HowStuffWorks, 2000) HowStuffWorks. *Why do batteries seem to go dead and then come back to life if you let them rest?*, http://electronics.howstuffworks.com/question390.htm.

(Huggins, 2008) R. Huggins. *Advanced Batteries: Materials Science Aspects*, 1st ed., Springer, 2008.

(Jaworski, 1999) R. K. Jaworski. Statistical Parameters Model for Predicting Time to Failure of Telecommunications Batteries, *in Proceedings of 21st International Telecommunications Energy Conference, INTELEC*, 1999.

(Kozlowski, 2003) J. D. Kozlowski. Electrochemical Cell Prognostics Using Online Impedance

Measurements and Model-based Data Fusion Techniques, *in Proceedings of IEEE Aerospace Conference 2003*, vol.7 pp. 3257-3270, 2003.

(Meissner and Richter, 2003) E. Meissner and G. Richter. Battery Monitoring and Electrical Energy Management - Precondition for Future Vehicle Electric Power Systems, *Journal of Power Sources*, vol. 116, no. 1, pp. 79-98, 2003.

(PKIDs, 2009) PKIDs. *PKIDs goes Green*, PKIDs Online, http://www.pkids.org/ap_green.php.

(Plett, 2004) G. L. Plett. Extended Kalman Filtering for Battery Management Systems of LiPB-based HEV Battery Packs, Parts 1–3, *Journal of Power Sources*, vol. 134, issue 2, pp. 252–292, 2004.

(Rufus *et al*., 2008) F. Rufus, S. Lee, and A. Thakker. Health Monitoring Algorithms for Space Application Batteries, *in Proceedings of International Conference on Prognostics and Health Management, 2008, PHM 2008*, Denver, CO, Oct 2008.

(Saha *et al*., 2009) B. Saha, K. Goebel, S. Poll, and J. Christophersen. Prognostics Methods for Battery Health Monitoring Using a Bayesian Framework, *IEEE Transactions on Instrumentation and Measurement,* vol.58, no.2, pp. 291-296, 2009.

(Santhanagopalan *et al*., 2008) S. Santhanagopalan, Q. Zhang, K. Kumaresan, and R. E. White. Parameter Estimation and Life Modeling of Lithium-Ion Cells, *Journal of The Electrochemical Society*, vol. 155, no. 4, pp. A345-A353, 2008.

(Saxena *et al*., 2008) A. Saxena, J. Celaya, E. Balaban, K. Goebel, B. Saha, S Saha, and M. Schwabacher. Metrics for Evaluating Performance of Prognostic Techniques, *in Proceedings of Intl. Conf. on Prognostics and Health Management*, Denver, CO, Oct 2008.

(Stamps *et al*., 2005) A. T. Stamps, C. E. Holland, R. E. White, and E. P. Gatzke. "Analysis of Capacity Fade in a Lithium Ion Battery." *Journal of Power Sources*, vol. 150, pp. 229-239, 2005.

(Vutetakis and Viswanathan, 1995) D. G. Vutetakis and V. V. Viswanathan. Determining the State-of-Health of Maintenance-Free Aircraft Batteries, *in Proceedings of Tenth Annual Battery Conference on Applications and Advances, Proceedings*, pp. 13-18, 1995.

Bhaskar Saha received his Ph.D. from the School of Electrical and Computer Engineering at Georgia Institute of Technology, Atlanta, GA, USA in 2008. He received his M.S. also from the same school and his B. Tech. (Bachelor of Technology) degree from the Department of Electrical Engineering, Indian Institute of Technology, Kharagpur, India. He is currently a Research Scientist with Mission Critical Technologies at the Prognostics Center of Excellence, NASA Ames Research Center. His research is focused on applying various classification, regression and state estimation techniques for predicting remaining useful life of systems and their components, as well as developing hardware-in-the-loop testbeds and prognostic metrics to evaluate their performance. He has been an IEEE member since 2008 and has published several papers on these topics.

Kai Goebel received the degree of Diplom-Ingenieur from the Technische Universität München, Germany in 1990. He received the M.S. and Ph.D. from the University of California at Berkeley in 1993 and 1996, respectively. Dr. Goebel is a senior scientist at NASA Ames Research Center where he leads the Diagnostics & Prognostics groups in the Intelligent Systems division. In addition, he directs the Prognostics Center of Excellence and he is the Associate Principal Investigator for Prognostics of NASA's Integrated Vehicle Health Management Program. He worked at General Electric's Corporate Research Center in Niskayuna, NY from 1997 to 2006 as a senior research scientist. He has carried out applied research in the areas of artificial intelligence, soft computing, and information fusion. His research interest lies in advancing these techniques for real time monitoring, diagnostics, and prognostics. He holds eleven patents and has published more than 100 papers in the area of systems health management.